

1 Cortical processing of breathlessness in the athletic brain

2 Olivia K. Faull^{1,2,3}, Pete J. Cox³, Kyle T. S. Pattinson^{1,2}

3

4 ¹FMRIB Centre and ²Nuffield Division of Anesthetics, Nuffield Department of Clinical
5 Neurosciences, University of Oxford, Oxford, UK, and ³Department of Physiology, Anatomy
6 and Genetics, University of Oxford, Oxford, UK

7

8

9 Running title: Athlete breathlessness brain networks

10 Key words: fMRI, ventilation, interoception, breathlessness, athletes

11

12

13 **Corresponding author:**

14 Dr Olivia Faull

15 Nuffield Department of Clinical Neurosciences

16 University of Oxford

17 Oxford, UK

18 Email: olivia.faul@ndcn.ox.ac.uk

19 Phone: +44 (0)1865 34544

20 Fax: +44 (0)1865 23079

21

22

23 **Key points**

- 24 • Endurance athletes train to improve their respiratory system for enhanced exercise
25 capacity and performance. However, it is unknown whether concurrent adaptation occurs
26 in brain networks perceiving respiratory-related sensations, such as breathlessness.
- 27 • We have previously shown improved matching between changes in ventilation and
28 perceptions of breathlessness in endurance athletes compared to sedentary controls (Faull
29 *et al.*, 2016a). Here, we used functional brain scanning to investigate differences in brain
30 activity during breathlessness tasks in these subjects.
- 31 • Athletes demonstrated a network of brain activity during anticipation of resistive
32 inspiratory loading that corresponds to subjective breathlessness intensity, which was
33 absent in sedentary controls. This may be related to improved brain synchronicity
34 observed between primary sensorimotor cortices and task-positive brain networks in
35 these athletes, and may underpin our previous findings of improved ventilatory
36 interoception.
- 37 • Understanding brain changes in respiratory perceptions may help us to target both
38 endurance training mechanisms and treatment of disease-related breathlessness
39 symptomology.

40 **Abstract**

41 Exercise is associated with large increases in ventilation, which are consciously perceived as the
42 sensation of breathlessness. We have previously demonstrated closer matching between changes
43 in ventilation and corresponding perceptions of breathlessness in endurance athletes compared
44 with sedentary controls (Faull *et al.*, 2016a), suggesting improved accuracy when interpreting
45 respiratory sensations, or ventilatory interoception. Here, we sought to identify the mechanisms
46 by which the processing of respiratory perception is optimised in these subjects.

47 Forty participants (20 athletes, 20 age/sex-matched sedentary participants) were scanned
48 using a 7T Siemens Magnetom (Nova Medical 32 channel Rx, single channel birdcage Tx).
49 Anticipation and breathlessness were induced with a previously trained delay-conditioned cue
50 and an inspiratory resistance during fMRI scanning. Differences between group means and slope
51 of subjective scores during task-based and resting fMRI were analysed using non-parametric
52 statistical testing and independent component analysis.

53 Athletes demonstrated greater brain activity corresponding with intensity scores during
54 anticipation of breathlessness, compared to sedentary controls. Athletes also exhibited greater
55 functional connectivity (or communication) between a task-positive brain network closely
56 matching breathlessness activity, and areas of primary sensorimotor cortices active during
57 inspiratory resistance. These functional activity and connectivity differences in athletic brains
58 may represent optimized processing of respiratory sensations, and contribute to improved
59 ventilatory interoception in athletes. Furthermore, these brain mechanisms may be harnessed
60 when exercise is employed in the treatment of breathlessness for chronic respiratory disease.

61 **Introduction**

62 Athletes are able to undertake incredible feats of human achievement, with faster, higher and
63 stronger performances recorded each year. Whilst exercise training is known to induce
64 widespread physiological changes in the periphery, the concurrent changes in the structure and
65 function of the athletic brain are less well investigated. For endurance athletes, exercise training
66 is targeted to improve the ability of tissues to utilize oxygen in the combustion of fuels such as
67 fat and carbohydrate, producing the energy required for repeated skeletal muscle contraction
68 (Holloszy & Coyle, 1984; Jones AM, 2012). However, the role of the brain in perceiving and
69 modulating changing sensations from the periphery, useful for processes such as pacing
70 strategies and to maintain homeostasis, is often overlooked.

71 Ventilation during exercise is tightly controlled, balancing neurally-modulated feed
72 forward ventilatory commands and peripheral feedback to stimulate appropriate ventilation for
73 exercising needs (Kaufman & Forster, 1996; Waldrop *et al.*, 1996). Respiratory sensations are
74 monitored to maintain homeostasis (Davenport & Vovk, 2009), and with sufficient exercise
75 intensity, the strain of immense increases in ventilation induces perceptions of breathlessness
76 (El-Manshawi *et al.*, 1986; Takano *et al.*, 1997; Lansing *et al.*, 2000; Borg *et al.*, 2010). While
77 endurance athletes are repeatedly exposed to these respiratory sensations and breathlessness, it is
78 as yet unknown whether brain networks involved in these perceptions may also adapt to better
79 cope with exercise demands. This understanding would allow us to explore how interoceptive
80 processing of ventilation might adapt or be altered in different states, such as here in athletes, and
81 open the door to future work in disease models of altered breathlessness perceptions.

82 Importantly, prior experiences of strong respiratory sensations may also alter the way
83 someone anticipates and perceives breathlessness (Faull *et al.*, 2017; Van den Bergh *et al.*, 2017;

84 Herigstad *et al.*, n.d.). Expectations regarding upcoming respiratory sensations from conditioned
85 cues (Pavlov *et al.*, 2003), for example the breathlessness associated with an approaching hill
86 whilst running, can be an important influence on both preventative actions (i.e. to avoid the hill),
87 or on the perception itself (Price *et al.*, 1999; Porro *et al.*, 2002; Wager *et al.*, 2004). Repeated
88 breathlessness exposure may alter this anticipation in athletes, focusing their attention towards
89 respiratory sensations (Merikle & Joordens, 1997; Phelps *et al.*, 2006; Ling & Carrasco, 2006),
90 reducing their anxiety (Spinhoven *et al.*, 1997; Bogaerts *et al.*, 2005; Tang & Gibson, 2005) or
91 improving their interoceptive ability (Gray *et al.*, 2007; Critchley *et al.*, 2013; Mallorqui-Bague
92 *et al.*, 2016; Garfinkel *et al.*, 2016b; 2016a). Interestingly, exercise therapy is currently the most
93 effective treatment for breathlessness associated with chronic obstructive pulmonary disease
94 (COPD), improving breathlessness intensity and anxiety (Carrieri-Kohlman *et al.*, 1996; 2001;
95 Herigstad *et al.*, n.d.), without concurrent improvements in lung function. It is possible that
96 athletes may have different prior expectations and anticipations of breathlessness, although this
97 has yet to be investigated.

98 In previous work we have observed closer matching between changes in ventilation and
99 perceptions of breathlessness in endurance athletes compared to sedentary individuals (Faull *et*
100 *al.*, 2016a). Here, we sought to identify how the brain processing of both anticipation and
101 perception of respiratory sensations may be altered in these athletes, to better understand
102 potential contributors to ventilatory interoception. We investigated functional brain activity
103 during both conditioned anticipation and perception of a breathlessness stimulus, as well as any
104 differences in the resting temporal coherence, or ‘functional connectivity’ (Gerstein & Perkel,
105 1969; Van Den Heuvel & Pol, 2010) of brain networks involved in attention towards sensory
106 information. Differences in underlying functional connectivity may help us to understand how

107 the athlete brain may be altered to facilitate accurate respiratory perceptions, and we
108 hypothesized that these athletes (Faull *et al.*, 2016a) would demonstrate both altered functional
109 breathlessness-related brain activity and connectivity to their sedentary counterparts.

110

111

112 **Materials and Methods**

113 **Subjects**

114 The Oxfordshire Clinical Research Ethics Committee approved the study and volunteers gave
115 written, informed consent. Forty healthy, right-handed individuals undertook this study (20
116 males, 20 females; mean age \pm SD, 26 ± 7 years), with no history of smoking or any respiratory
117 disease. This cohort comprised two groups; 20 subjects who regularly participated in endurance
118 sport (10 males, 10 females; mean age \pm SEM, 26 ± 1.7 years) and 20 age- and sex-matched (± 2
119 years) sedentary subjects (10 males, 10 females; mean age \pm SEM, 26 ± 1.7 years). Prior to
120 scanning, all subjects underwent breathlessness testing during exercise and chemostimulated
121 hyperpnea, which have been presented elsewhere (Faull *et al.*, 2016a), and a combined whole-
122 group analysis of fMRI data has been previously reported (Faull & Pattinson, 2017).

123

124 **Stimuli and tasks**

125 Subjects were trained using an aversive delay-conditioning paradigm to associate simple shapes
126 with an upcoming breathlessness (inspiratory resistance) stimulus (Faull & Pattinson, 2017).
127 Two conditions were trained: 1) A shape that always predicted upcoming breathlessness (100%
128 contingency pairing), and 2) A shape that always predicted unloaded breathing (0% contingency
129 pairing with inspiratory resistance). The 'certain upcoming breathlessness' symbol was presented

130 on the screen for 30 s, which included a varying 5-15 s anticipation period before the loading
131 was applied. The 'unloaded breathing' symbol was presented for 20 s, and each condition was
132 repeated 14 times in a semi-randomised order. A finger opposition task was also included in the
133 protocol, where an opposition movement was conducted between the right thumb and fingers,
134 with the cue 'TAP' presented for 15 s (10 repeats). Conscious associations between cue and
135 threat level (cue contingencies) were required and verified in all subjects by reporting the
136 meaning of each of the symbols following the training session and immediately prior to the MRI
137 scan.

138 Rating scores of breathing perceptions were recorded after every symbol and at the
139 beginning and end of the task, using a visual-analogue scale (VAS) with a sliding bar to answer
140 the question 'How difficult was the previous stimulus?' where the subjects moved between 'Not
141 at all difficult' (0%) and 'Extremely difficult' (100%). Subjects were also asked to rate how
142 anxious each of the symbols made them feel ('How anxious does this symbol make you feel?')
143 using a VAS between 'Not at all anxious' (0%) and 'Extremely anxious' (100%) immediately
144 following the functional MRI protocol.

145

146 **Breathing system and Physiological measurements**

147 A breathing system was used to remotely administer periods of inspiratory resistive loading to
148 induce breathlessness (as predicted by the conditioned cues), as previously described (Faull *et al.*,
149 2016b). End-tidal oxygen and carbon dioxide were maintained constant. The subject's nose was
150 blocked using foam earplugs and they were asked to breathe through their mouth for the duration
151 of the experiment. Physiological measures were recorded continuously during the training
152 session and MRI scan as previously described (Faull *et al.*, 2016b).

153

154 **MRI scanning sequences**

155 MRI was performed with a 7 T Siemens Magnetom scanner, with 70 mT/m gradient strength and
156 a 32 channel Rx, single channel birdcage Tx head coil (Nova Medical).

157 *BOLD scanning:* A T2*-weighted, gradient echo EPI was used for functional scanning.
158 The field of view (FOV) covered the whole brain and comprised 63 slices (sequence parameters:
159 TE, 24 ms; TR, 3 s; flip angle, 90°; voxel size, 2 x 2 x 2 mm; field of view, 220 mm; GRAPPA
160 factor, 3; echo spacing, 0.57 ms; slice acquisition order, descending), with 550 volumes (scan
161 duration, 27 mins 30 s) for the task fMRI, and 190 volumes (scan duration, 9 mins 30 s) for a
162 resting-state acquisition (eyes open).

163 *Structural scanning:* A T1-weighted structural scan (MPRAGE, sequence parameters:
164 TE, 2.96 ms; TR, 2200 ms; flip angle, 7°; voxel size, 0.7 x 0.7 x 0.7 mm; field of view, 224 mm;
165 inversion time, 1050 ms; bandwidth; 240 Hz/Px) was acquired. This scan was used for
166 registration of functional images.

167 *Additional scanning:* Fieldmap scans (sequence parameters: TE1, 4.08 ms; TE2, 5.1 ms;
168 TR, 620 ms; flip angle, 39°; voxel size, 2 x 2 x 2 mm) of the B₀ field were also acquired to assist
169 distortion-correction.

170

171 **Physiological data analysis**

172 Values for mean and peak resistive loading, mean P_{ET}CO₂, P_{ET}O₂, respiratory rate and
173 respiratory volume per unit time (RVT) were calculated across each time block using custom
174 written scripts in MATLAB (R2013a, The Mathworks, Natick, MA). Measures were averaged
175 across each subject in each condition (unloaded breathing, anticipation and breathlessness). Peak

176 mouth pressure was also calculated in each block and averaged in each subject for the resistive
177 loading condition. Mean peak mouth pressure, breathlessness intensity and breathlessness
178 anxiety ratings were then compared between the two groups using a student's paired T-test.

179

180 **Imaging analysis**

181 *Preprocessing:* Image processing was performed using the Oxford Centre for Functional
182 Magnetic Resonance Imaging of the Brain Software Library (FMRIB, Oxford, UK; FSL version
183 5.0.8; <http://www.fmrib.ox.ac.uk/fsl/>). The following preprocessing methods were used prior to
184 statistical analysis: motion correction and motion parameter recording (MCFLIRT (Jenkinson *et*
185 *al.*, 2002)), removal of the non-brain structures (skull and surrounding tissue) (BET (Smith,
186 2002)), spatial smoothing using a full-width half-maximum Gaussian kernel of 2 mm, and high-
187 pass temporal filtering (Gaussian-weighted least-squares straight line fitting; 120 s). B₀ field
188 unwarping was conducted with a combination of FUGUE and BBR (Boundary-Based-
189 Registration; part of FEAT: FMRI Expert Analysis Tool, version 6.0 (Greve & Fischl, 2009)).
190 Data denoising was conducted using a combination of independent components analysis (ICA)
191 and retrospective image correction (RETROICOR) (Harvey *et al.*, 2008; Brooks *et al.*, 2013), as
192 previously described (Faull *et al.*, 2016b).

193 *Image registration:* Following preprocessing, the functional scans were registered to the
194 MNI152 (1x1x1 mm) standard space (average T1 brain image constructed from 152 normal
195 subjects at the Montreal Neurological Institute (MNI), Montreal, QC, Canada) using a two-step
196 process: 1) Registration of subjects' whole-brain EPI to T1 structural image was conducted using
197 BBR (6 DOF) with (nonlinear) fieldmap distortion-correction (Greve & Fischl, 2009), and 2)

198 Registration of the subjects' T1 structural scan to 1 mm standard space was performed using an
199 affine transformation followed by nonlinear registration (FNIRT) (Andersson *et al.*, 2007).

200 *Functional voxelwise and group analysis:* Functional data processing was performed
201 using FEAT (fMRI Expert Analysis Tool), part of FSL. The first-level analysis in FEAT
202 incorporated a general linear model (Woolrich *et al.*, 2004), with the following regressors:
203 Breathlessness periods (calculated from physiological pressure trace as onset to termination of
204 each application of resistance); anticipation of breathlessness (calculated from onset of
205 anticipation symbol to onset of resistance application); unloaded breathing (onset and duration of
206 'unloaded breathing' symbol); and finger opposition (onset and duration of finger opposition
207 screen instruction). Additional regressors to account for relief from breathlessness, periods of
208 rating using the button box, demeaned ratings of intensity between trials, and a period of no
209 loading following the final anticipation period (for decorrelation between anticipation and
210 breathlessness) were also included in the analysis. A final $P_{ET}CO_2$ regressor was formed by
211 linearly extrapolating between end-tidal CO_2 peaks, and included in the general linear model to
212 decorrelate any $P_{ET}CO_2$ -induced changes in BOLD signal from the respiratory tasks (McKay *et*
213 *al.*, 2008; Pattinson *et al.*, 2009a; 2009b; Faull *et al.*, 2015; 2016b). Contrasts for breathlessness
214 (vs. baseline) and differential contrasts of anticipation of breathlessness > unloaded breathing
215 (referred to as 'anticipation' or 'anticipation of breathlessness') were investigated at the group
216 level, as well as the control condition of finger opposition (vs. baseline).

217 Functional voxelwise analysis incorporated HRF modeling using three FLOBS regressors
218 to account for any HRF differences caused by slice-timing delays, differences across the
219 brainstem and cortex, or between individuals (Handwerker *et al.*, 2004; Devonshire *et al.*, 2012).
220 Time-series statistical analysis was performed using FILM, with local autocorrelation correction

221 (Woolrich *et al.*, 2001). The second and third waveforms were orthogonalised to the first to
222 model the ‘canonical’ HRF, of which the parameter estimate was then passed up to the group
223 analysis in a mixed-effects analysis. Group analysis was conducted using rigorous permutation
224 testing of a General Linear Model (GLM) using FSL’s Randomize tool (Winkler *et al.*, 2014),
225 where the GLM consisted of group mean BOLD activity for each group, and demeaned,
226 separated breathlessness intensity and anxiety covariates for each group. Voxelwise differences
227 between mean group activity were calculated, as well as the interactions between group and
228 breathlessness intensity / anxiety scores. A stringent initial cluster-forming threshold of $t = 3.1$
229 was used, in light of recent reports of lenient thresholding previously used in fMRI (Eklund *et al.*,
230 2016), and images were family-wise-error (FWE) corrected for multiple comparisons.
231 Significance was taken at $p < 0.05$ (corrected).

232 *Resting functional connectivity analysis:* Following preprocessing and image registration,
233 resting state scans from all subjects were temporally concatenated and analysed using
234 independent component analysis (ICA) using MELODIC (Beckmann & Smith, 2004), part of
235 FSL. ICA decomposes the data into a set of spatial maps and their associated timecourses,
236 referred to as ‘functional networks’. Model order in the group ICA was set to 25 spatially
237 independent components. Dual regression (Beckmann *et al.*, 2009) was then used to delineate
238 subject-specific timecourses of these components, and their corresponding subject-specific
239 spatial maps. Subject-specific spatial maps were again analysed non-parametrically using
240 Randomise (part of FSL) (Winkler *et al.*, 2014) with the same GLM and significance thresholds
241 previously applied to the functional task group analysis. Twenty components were identified as
242 signal, and two components of interest (‘default mode’ network and ‘task positive’ network)

243 were considered for group differences. Therefore, p threshold significance was adjusted to $p <$
244 0.025 using Bonferroni correction for multiple comparisons.

245

246

247 **Results**

248 **Physiology and psychology of breathlessness**

249 Mean physiological values for each group for mouth pressure, $P_{ET}CO_2$, $P_{ET}O_2$, RVT, respiratory
250 rate and RVT are presented in Table 1. Group scores for breathlessness intensity and anxiety are
251 presented in Table 2, with no mean differences observed between groups.

252

253 **Task fMRI analysis**

254 *Anticipation of breathlessness:* Mean activity during anticipation of breathlessness in each group
255 is presented in Figure 1. In sedentary subjects, significantly increased BOLD activity was
256 observed in the right anterior insula, operculum and bilateral primary motor cortex, and
257 decreased BOLD activity in bilateral posterior cingulate cortex, precuneus, lateral occipital
258 cortex, hippocampus, parahippocampal gyrus and amygdala. In athletes, increased BOLD
259 activity was observed in bilateral anterior insula, operculum and primary motor cortex, and right
260 supplementary motor cortex, and decreased BOLD activity in bilateral precuneus, hippocampus,
261 parahippocampal gyrus and amygdala. No statistically significant voxelwise differences were
262 observed between group mean activities during anticipation of breathlessness (differentially
263 contrasted against unloaded breathing).

264 *Resistive loading:* Mean activity during breathlessness in each group is presented in
265 Figure 1. In sedentary subjects, significantly increased BOLD activity was observed in the

266 bilateral anterior and middle insula, operculum, primary sensory and motor cortices,
267 supplementary motor cortex, supramarginal gyrus and cerebellar VI, and decreased BOLD
268 activity in bilateral precuneus. In athletes, significantly increased BOLD activity was observed in
269 the right dorsolateral prefrontal cortex, bilateral anterior and middle insula, operculum, primary
270 sensory and motor cortices, supplementary motor cortex, left visual cortex and cerebellar Crus-I,
271 and decreased BOLD activity in right amygdala, hippocampus and superior temporal gyrus. No
272 statistically significant voxelwise differences were observed between group mean activities
273 during breathlessness.

274 *Subjective breathlessness scores:* Brain activity that correlated with breathlessness scores
275 of intensity and anxiety were compared between groups. Athletes demonstrated widespread brain
276 activity positively correlating with intensity scores during anticipation of breathlessness (Figure
277 2), whilst those same areas had a negative correlation in sedentary subjects (interaction). This
278 included activity in the bilateral ventral posterolateral nucleus of the thalamus, middle insula,
279 and primary motor and sensory cortices, as well as left anterior insula. In contrast, a small
280 amount of activity in the right putamen and caudate nucleus correlated with anxiety in sedentary
281 subjects, but not in athletes during anticipation. No significant interactions between groups were
282 present for either intensity of anxiety during breathlessness perception.

283 *Finger opposition:* Results of the control finger opposition task are provided in the
284 Supplementary material.

285

286 **Resting state network connectivity**

287 Of the 25 resting state ‘networks’ identified in the group ICA analysis, 20 components were
288 identified to represent relevant signal (19 cortical, 1 cerebellar) while the remaining 5 were

289 labeled as noise (see Supplementary Figure 1 for a summary the 20 resting networks). Two
290 networks of interest were identified for group comparison analyses: 1) The network most
291 representative of the typical ‘default mode’, which was closely represented by the whole group
292 decrease in brain activity during anticipation of breathlessness, and 2) The network that
293 displayed the most similarity to the task contrasts (anticipation and resistive loading) or ‘task-
294 positive’ network, containing components of previously identified visual and dorsal attention
295 networks (Vossel *et al.*, 2014) (Figure 3). When network connectivity was compared between
296 athletes and controls, athletes were found to have significantly greater ($p = 0.019$) connectivity of
297 the task-positive network to an area of primary motor cortex active during resistive loading
298 (Figure 3).

299

300

301 **Discussion**

302 **Main findings**

303 We have identified a cohesive brain network pertaining to subjective ratings of anticipated
304 breathlessness intensity in athletes, which is absent in sedentary controls. Comparatively,
305 sedentary subjects demonstrated anticipatory activity in the caudate nucleus and putamen
306 corresponding to anxiety scores, which was not present in athletes. Athletes also demonstrated
307 greater connectivity between an area of primary sensorimotor cortex that is active during
308 inspiratory resistance, and a cingulo-opercular ‘task-positive’ network identified at rest. This
309 network has strikingly similarities to the pattern of positive and negative BOLD changes induced
310 during both anticipation and breathlessness, and may relate to attention and processing of
311 sensory signals related to breathlessness. Increased connectivity between sensorimotor cortex

312 and the cingulo-opercular brain areas active during breathlessness tasks may underlie the
313 observed differences in processing of respiratory signals during anticipation, and the improved
314 ventilatory interoception previously reported in these endurance athletes (Faull *et al.*, 2016a).

315

316 **Breathlessness processing in athletes**

317 Endurance athletes have repeatedly elevated ventilation and perceptions of breathlessness as part
318 of their training. In previously published results (Faull *et al.*, 2016a), we have demonstrated
319 improved psychophysical matching between changes in chemostimulated hyperventilation and
320 subjective breathlessness perceptions in these athletes compared to matched sedentary subjects.
321 Therefore, whether by nature or nurture, these individuals appear to have improved ventilatory
322 perception accuracy. A random relationship between changes in ventilation and perceptions of
323 breathlessness (demonstrated in sedentary subjects) implies a worsened ability to process
324 respiratory sensations, which may be a risk factor for symptom discordance in disease (Van den
325 Bergh *et al.*, 2017). Accordingly, a coherent network of brain activity was present corresponding
326 to breathlessness intensity scores in athletes, incorporating key areas involved in sensorimotor
327 control and interoception, such as the thalamus, insula and primary sensorimotor cortices
328 (Feldman & Friston, 2010; Simmons *et al.*, 2012; Barrett & Simmons, 2015; Van den Bergh *et*
329 *al.*, 2017). Conversely, sedentary subjects demonstrated activity corresponding to anxiety scores
330 in the ventral striatum (caudate nucleus and putamen) during anticipation of breathlessness. The
331 striatum has been previously linked with cardiovascular responses resulting from social threat
332 (Wager *et al.*, 2009), and may represent heightened threat responses in sedentary subjects.

333 Interestingly, the intensity-related differences in brain activity were observed during the
334 anticipation period preceding the actual perception of breathlessness. It is possible that repeated

335 increases in ventilation and breathlessness during training helps athletes improve the accuracy of
336 their breathing expectations for an upcoming stimulus, such as expecting to run up a hill. Recent
337 theories of symptom perception have proposed a comprehensive, Bayesian model (Barrett &
338 Simmons, 2015; Van den Bergh *et al.*, 2017), which includes a set of perceptual expectations or
339 ‘priors’. These expectations are combined with sensory information from the periphery, for the
340 brain to probabilistically produce the most likely resulting perception. Furthermore, factors such
341 as attention (Merikle & Joordens, 1997; Phelps *et al.*, 2006; Ling & Carrasco, 2006) and
342 interoceptive ability (Gray *et al.*, 2007; Critchley *et al.*, 2013; Mallorqui-Bague *et al.*, 2016;
343 Garfinkel *et al.*, 2016b) are thought to influence this system, either by altering the prior
344 expectations or incoming sensory information. Therefore, it is possible that repeated exercise
345 training in athletes could develop breathlessness expectations (or priors) and direct attention
346 towards breathing sensations, improving the robustness of the perceptual system to accurately
347 infer the intensity of breathlessness.

348

349 **Differences in functional connectivity within the athletic brain**

350 Understanding differences in underlying communication between functional brain regions may
351 inform us as to why differences in functional activity, such as observed in these athletes during
352 anticipation of breathlessness, may arise. The temporal synchronicity of seemingly spontaneous
353 fluctuations in brain activity across spatially distinct regions can inform us of how ‘functionally
354 connected’ these disparate regions may be, and is thought to be related to the temporal coherence
355 of neuronal activity in anatomically distinct areas (Gerstein & Perkel, 1969; Van Den Heuvel &
356 Pol, 2010).

357 It is now well established that the brain can be functionally parsed into resting state
358 ‘networks’, where distinct brain regions are consistently shown to exhibit temporally similar
359 patterns of brain activity (Smith *et al.*, 2009; Miller *et al.*, 2016). While properties of these
360 resting state networks have been linked to lifestyle, demographic and psychometric factors
361 (Smith *et al.*, 2015; Miller *et al.*, 2016), here we have found connectivity differences between
362 athletes and sedentary subjects for a cingulo-opercular network that displays a very similar
363 spatial distribution to the pattern of activity observed during the breathlessness tasks (‘task-
364 positive’), with (on average) a negative connectivity to primary sensorimotor cortices active
365 during breathlessness (Figure 3). This task-positive network is also strikingly similar to
366 previously reported networks of ventral and dorsal attention (Fox *et al.*, 2005; 2006). Here, we
367 have demonstrated greater functional connectivity in athletes between an area of primary sensory
368 and motor cortices that has consistently been identified as active during tasks such as breath
369 holds (Pattinson *et al.*, 2009b; Faull *et al.*, 2015) and inspiratory resistances (Faull *et al.*, 2016b;
370 Hayen *et al.*, 2017; Faull & Pattinson, 2017). It is possible that this greater connectivity in
371 athletes between an attention network and primary sensorimotor cortex contributes to the
372 processing of incoming and outgoing respiratory information, and thus may also be related to
373 improved ventilatory interoception.

374 Whilst this cross-sectional study is unable to determine whether endurance exercise
375 training *induces* these differences in brain function and connectivity, or whether these
376 individuals are biased towards training for endurance sports, this work provides intriguing
377 preliminary insight that the brain may undergo adaptation in conjunction with the periphery, to
378 more accurately process ventilatory interoception and perceptions of bodily sensations such as
379 breathlessness.

380

381 **Clinical implications of altering breathlessness processing**

382 As discussed, prior expectations of breathlessness are now considered to be a major contributor
383 to symptom perception (Hayen *et al.*, 2013; Faull *et al.*, 2017; Van den Bergh *et al.*, 2017;
384 Geuter *et al.*, 2017; Herigstad *et al.*, n.d.). Altering the accuracy of breathlessness perception
385 using exercise training may be of interest when treating individuals with habitual symptomology,
386 such as those with chronic obstructive pulmonary disease (COPD) or asthma. Recent research
387 has shown exercise training to reduce breathlessness intensity and anxiety in patients with
388 COPD, with corresponding changes in the brain's processing of breathlessness-related words
389 (Herigstad *et al.*, 2016; n.d.). It has been proposed that exercise exposure alters breathlessness
390 expectations and priors in these patients, modifying symptom perception when it has become
391 discordant with physiology in chronic disease (Parshall *et al.*, 2012; Herigstad *et al.*, n.d.). It is
392 also possible that exercise helps improve the processing of respiratory signals for more accurate
393 ventilatory interoception in these patients, allowing breathlessness perception to better match
394 respiratory distress. Future work investigating the link between exercise, ventilatory
395 interoception and breathlessness perception may yield another treatment avenue (via
396 interoception and more targeted exercise) to improve patient quality of life in the face of chronic
397 breathlessness.

398

399

400 **Conclusions**

401 In this study, we have demonstrated altered anticipatory brain processing of breathlessness
402 intensity in athletes compared to sedentary subjects. This altered functional brain activity may be

403 underpinned by increased functional connectivity between a task-positive network related to
404 breathlessness, and sensorimotor cortex that is active during ventilatory tasks. These differences
405 in brain activity and connectivity may relate to improvements in ventilatory interoception
406 previously reported between these subject groups (Faull *et al.*, 2016a), and open the door to
407 investigating exercise and interoception as a tool to manipulate brain processing of debilitating
408 symptoms, such as breathlessness in clinical populations.

409

410

411 **Acknowledgements**

412 This research was supported by the JABBS Foundation. This research was further supported by
413 the National Institute for Health Research, Oxford Biomedical Research Centre based at Oxford
414 University Hospitals NHS Trust and University of Oxford. Olivia K Faull was supported by the
415 Commonwealth Scholarship Commission. The authors would like to thank xxx for their thoughts
416 and comments on the manuscript.

417

418

419 **Competing interests**

420 KP has acted as a consultant for Nektar Therapeutics. The work for Nektar has no bearing on the
421 contents of this manuscript.

422

423

424 **References**

- 425 Andersson JL, Jenkinson M & Smith S (2007). Non-linear registration, aka Spatial normalisation
426 FMRIB technical report TR07JA2. *FMRIB Analysis Group of the University of Oxford*.
- 427 Barrett LF & Simmons WK (2015). Interoceptive predictions in the brain. *Nat Rev Neurosci* **16**,
428 419–429.
- 429 Beckmann CF & Smith SM (2004). Probabilistic Independent Component Analysis for
430 Functional Magnetic Resonance Imaging. *IEEE Transactions on Medical Imaging* **23**, 137–
431 152.
- 432 Beckmann CF, Mackay CE, Filippini N & Smith SM (2009). Group comparison of resting-state
433 FMRI data using multi-subject ICA and dual regression. *NeuroImage* **47**, S148.
- 434 Bogaerts K, Notebaert K, Van Diest I, Devriese S, De Peuter S & Van den Bergh O (2005).
435 Accuracy of respiratory symptom perception in different affective contexts. *J Psychosom*
436 *Res* **58**, 537–543.
- 437 Borg E, Borg G, Larsson K, Letzter M & Sundblad BM (2010). An index for breathlessness and
438 leg fatigue. *Scand J Med Sci Sports* **20**, 644–650.
- 439 Brooks JCW, Faull OK, Pattinson KTS & Jenkinson M (2013). Physiological noise in brainstem
440 FMRI. *Front Hum Neurosci* **7**, 623–13.
- 441 Carrieri-Kohlman V, Gormley JM, Douglas MK, Paul SM & Stulbarg MS (1996). Exercise
442 training decreases dyspnea and the distress and anxiety associated with it: monitoring alone
443 may be as effective as coaching. *Chest Journal* **110**, 1526–1535.
- 444 Carrieri-Kohlman V, Gormley JM, Eiser S, Demir-Deviren S, Nguyen H, Paul SM & Stulbarg
445 MS (2001). Dyspnea and the affective response during exercise training in obstructive
446 pulmonary disease. *Nursing Research* **50**, 136–146.
- 447 Critchley HD, Eccles J & Garfinkel SN (2013). Interaction between cognition, emotion, and the
448 autonomic nervous system. In *Autonomic Nervous System, Handbook of Clinical Neurology*,
449 pp. 59–77. Elsevier.
- 450 Davenport PW & Vovk A (2009). Cortical and subcortical central neural pathways in respiratory
451 sensations. *Respiratory physiology & neurobiology* **167**, 72–86.
- 452 Devonshire IM, Papadakis NG, Port M, Berwick J, Kennerley AJ, Mayhew JEW & Overton PG
453 (2012). Neurovascular coupling is brain region-dependent. *NeuroImage* **59**, 1997–2006.
- 454 Eklund A, Nichols TE & Knutsson H (2016). Cluster failure: Why fMRI inferences for spatial
455 extent have inflated false-positive rate. *PNAS* **113**, 7900–7905.
- 456 El-Manshawi A, Killian KJ, Summers E & Jones NL (1986). Breathlessness during exercise with
457 and without resistive loading. *Journal of Applied \ldots* **61**, 896–905.
- 458 Faull O, Hayen A & Pattinson K (2017). Breathlessness and the body: Neuroimaging clues for

- 459 the inferential leap. *Cortex*; DOI: 10.1101/117408.
- 460 Faull OK & Pattinson KT (2017). The cortical connectivity of the periaqueductal gray and the
461 conditioned response to the threat of breathlessness. *Elife* **6**, 95.
- 462 Faull OK, Cox PJ & Pattinson KTS (2016a). Psychophysical Differences in Ventilatory
463 Awareness and Breathlessness between Athletes and Sedentary Individuals. *Front Physiol* **7**,
464 195–199.
- 465 Faull OK, Jenkinson M, Clare S & Pattinson KTS (2015). Functional subdivision of the human
466 periaqueductal grey in respiratory control using 7 tesla fMRI. *NeuroImage* **113**, 356–364.
- 467 Faull OK, Jenkinson M, Ezra M & Pattinson KTS (2016b). Conditioned respiratory threat in the
468 subdivisions of the human periaqueductal gray. *Elife*; DOI: 10.7554/elife.12047.
- 469 Feldman H & Friston KJ (2010). Attention, Uncertainty, and Free-Energy. *Front Hum Neurosci*
470 **4**, 1–23.
- 471 Fox MD, Corbetta M, Snyder AZ, Vincent JL & Raichle ME (2006). Spontaneous neuronal
472 activity distinguishes human dorsal and ventral attention systems (vol 103, pg 10046, 2006).
473 *Proceedings of the National Academy of Sciences* **103**, 13560–13560.
- 474 Fox MD, Snyder AZ, Vincent JL, Corbetta M, Van Essen DC & Raichle ME (2005). The human
475 brain is intrinsically organized into dynamic, anticorrelated functional networks.
476 *Proceedings of the National Academy of Sciences* **102**, 9673–9678.
- 477 Garfinkel SN, Manassei MF, Hamilton-Fletcher G, In den Bosch Y, Critchley HD & Engels M
478 (2016a). Interoceptive dimensions across cardiac and respiratory axes. *Philos Trans R Soc
479 Lond, B, Biol Sci* **371**, 20160014–10.
- 480 Garfinkel SN, Tiley C, O'Keefe S, Harrison NA, Seth AK & Critchley HD (2016b).
481 Discrepancies between dimensions of interoception in autism: Implications for emotion and
482 anxiety. *Biological Psychology* **114**, 117–126.
- 483 Gerstein GL & Perkel DH (1969). Simultaneously recorded trains of action potentials: analysis
484 and functional interpretation. *Science* **164**, 828–830.
- 485 Geuter S, Boll S, Eippert F & Büchel C (2017). Functional dissociation of stimulus intensity
486 encoding and predictive coding of pain in the insula. *Elife* **6**, e24770.
- 487 Gray MA, Harrison NA, Wiens S & Critchley HD (2007). Modulation of Emotional Appraisal
488 by False Physiological Feedback during fMRI. *PLoS ONE* **2**, e546.
- 489 Greve DN & Fischl B (2009). Accurate and robust brain image alignment using boundary-based
490 registration. *NeuroImage* **48**, 63–72.
- 491 Handwerker DA, Ollinger JM & D'Esposito M (2004). Variation of BOLD hemodynamic
492 responses across subjects and brain regions and their effects on statistical analyses.

- 493 *NeuroImage* **21**, 1639–1651.
- 494 Harvey AK, Pattinson KTS, Brooks JCW, Mayhew SD, Jenkinson M & Wise RG (2008).
495 Brainstem functional magnetic resonance imaging: Disentangling signal from physiological
496 noise. *Journal of Magnetic Resonance Imaging* **28**, 1337–1344.
- 497 Hayen A, Herigstad M & Pattinson KTS (2013). Understanding dyspnea as a complex individual
498 experience. *Maturitas* **76**, 45–50.
- 499 Hayen A, Wanigasekera V, Faull OK, Campbell SF, Garry PS, Raby SJM, Robertson J, Webster
500 R, Wise RG, Herigstad M & Pattinson KTS (2017). Opioid suppression of conditioned
501 anticipatory brain responses to breathlessness. *NeuroImage* 1–44.
- 502 Herigstad M, Faull O, Hayen A, Evans E, Hardinge M, Wiech K & Pattinson KTS (n.d.).
503 Treating breathlessness via the brain: Mechanisms underpinning improvements in
504 breathlessness with pulmonary rehabilitation. *European Respiratory Journal*; DOI:
505 10.1101/117390.
- 506 Herigstad M, Hayen A, Reinecke A & Pattinson KTS (2016). Development of a dyspnoea word
507 cue set for studies of emotional processing in COPD. *Respiratory physiology &*
508 *neurobiology* **223**, 37–42.
- 509 Holloszy JO & Coyle EF (1984). Adaptations of Skeletal-Muscle to Endurance Exercise and
510 Their Metabolic Consequences. *Journal of Applied Physiology* **56**, 831–838.
- 511 Jenkinson M, Bannister P, Brady M & Smith S (2002). Improved Optimization for the Robust
512 and Accurate Linear Registration and Motion Correction of Brain Images. *NeuroImage* **17**,
513 825–841.
- 514 Jones AM CH (2012). The Effect of Endurance Training on Parameters of Aerobic Fitness. 1–14.
- 515 Kaufman MP & Forster HV (1996). Reflexes controlling circulatory, ventilatory and airway
516 responses to exercise.
- 517 Lansing RW, Im B, Thwing JI, Legedza A & Banzett RB (2000). The perception of respiratory
518 work and effort can be independent of the perception of air hunger. *Am J Respir Crit Care*
519 *Med* **162**, 1690–1696.
- 520 Ling S & Carrasco M (2006). When sustained attention impairs perception. *Nat Neurosci* **9**,
521 1243–1245.
- 522 Mallorqui-Bague N, Bulbena A, Pailhez G, Garfinkel SN & Critchley HD (2016). Mind-Body
523 Interactions in Anxiety and Somatic Symptoms. *Harvard Review of Psychiatry* **24**, 53–60.
- 524 McKay LC, Adams L, Frackowiak RSJ & Corfield DR (2008). A bilateral cortico-bulbar
525 network associated with breath holding in humans, determined by functional magnetic
526 resonance imaging. *NeuroImage* **40**, 1824–1832.

- 527 Merikle PM & Joordens S (1997). Parallels between Perception without Attention and
528 Perception without Awareness. *Consciousness and cognition* **6**, 219–236.
- 529 Miller KL et al. (2016). Multimodal population brain imaging in the UK Biobank prospective
530 epidemiological study. *Nat Neurosci* **19**, 1523–1536.
- 531 Parshall MB, Schwartzstein RM, Adams L, Banzett RB, Manning HL, Bourbeau J, Calverley
532 PM, Gift AG, Harver A, Lareau SC, Mahler DA, Meek PM & O'Donnell DE (2012). An
533 Official American Thoracic Society Statement: Update on the Mechanisms, Assessment, and
534 Management of Dyspnea. *Am J Respir Crit Care Med* **185**, 435–452.
- 535 Pattinson K, Mitsis GD, Harvey AK & Jbabdi S (2009a). Determination of the human brainstem
536 respiratory control network and its cortical connections in vivo using functional and
537 structural imaging. *NeuroImage* **44**, 295–305.
- 538 Pattinson KTS, Governo RJ, MacIntosh BJ, Russell EC, Corfield DR, Tracey I & Wise RG
539 (2009b). Opioids Depress Cortical Centers Responsible for the Volitional Control of
540 Respiration. *Journal of Neuroscience* **29**, 8177–8186.
- 541 Phelps EA, Ling S & Carrasco M (2006). Emotion facilitates perception and potentiates the
542 perceptual benefits of attention. *Psychol Sci* **17**, 292–299.
- 543 Porro CA, Baraldi P, Pagnoni G, Serafini M, Facchin P, Maieron M & Nichelli P (2002). Does
544 anticipation of pain affect cortical nociceptive systems? *The Journal of Neuroscience* **22**,
545 3206–3214.
- 546 Price DD, Milling LS, Kirsch I, Duff A, Montgomery GH & Nicholls SS (1999). An analysis of
547 factors that contribute to the magnitude of placebo analgesia in an experimental paradigm.
548 *Pain* **83**, 147–156.
- 549 Simmons WK, Avery JA, Barcalow JC, Bodurka J, Drevets WC & Bellgowan P (2012). Keeping
550 the body in mind: Insula functional organization and functional connectivity integrate
551 interoceptive, exteroceptive, and emotional awareness. *Human brain mapping* **34**, 2944–
552 2958.
- 553 Smith SM (2002). Fast robust automated brain extraction. *Human brain mapping* **17**, 143–155.
- 554 Smith SM, Fox PT, Miller KL, Glahn DC, Fox PM, Mackay CE, Filippini N, Watkins KE, Toro
555 R, Laird AR & Beckmann CF (2009). Correspondence of the brain's functional architecture
556 during activation and rest. 1–6.
- 557 Smith SM, Nichols TE, Vidaurre D, Winkler AM, Behrens TEJ, Glasser MF, Ugurbil K, Barch
558 DM, Van Essen DC & Miller KL (2015). A positive-negative mode of population
559 covariation links brain connectivity, demographics and behavior. *Nature Med* **18**, 1565–1567.
- 560 Spinhoven P, vanPeskiOosterbaan AS, VanderDoes A, Willems L & Sterk PJ (1997).
561 Association of anxiety with perception of histamine induced bronchoconstriction in patients
562 with asthma. *Thorax* **52**, 149–152.

- 563 Takano N, Inaishi S & Zhang Y (1997). Individual differences in breathlessness during exercise,
564 as related to ventilatory chemosensitivities in humans. *The Journal of Physiology* **499**, 843–
565 848.
- 566 Tang J & Gibson S (2005). A Psychophysical Evaluation of the Relationship Between Trait
567 Anxiety, Pain Perception, and Induced State Anxiety. *The Journal of Pain* **6**, 612–619.
- 568 Van den Bergh O, Witthöft M, Petersen S & Brown RJ (2017). Symptoms and the body: Taking
569 the inferential leap. *Neuroscience & Biobehavioral Reviews* **74**, 185–203.
- 570 Van Den Heuvel MP & Pol HEH (2010). Exploring the brain network: a review on resting-state
571 fMRI functional connectivity. *European Neuropsychopharmacology* **20**, 519–534.
- 572 Vossel S, Geng JJ & Fink GR (2014). Dorsal and Ventral Attention Systems: Distinct Neural
573 Circuits but Collaborative Roles. *neuroscientist* **20**, 150–159.
- 574 Wager TD, Rilling JK, Smith EE, Sokolik A, Casey KL, Davidson RJ, Kosslyn SM, Rose RM &
575 Cohen JD (2004). Placebo-Induced Changes in fMRI in the Anticipation and Experience of
576 Pain. *Science* **303**, 1162–1167.
- 577 Wager TD, Waugh CE, Lindquist M, Noll DC, Fredrickson BL & Taylor SF (2009). Brain
578 mediators of cardiovascular responses to social threat. *NeuroImage* **47**, 821–835.
- 579 Waldrop TG, Eldridge FL, Iwamoto GA & Mitchell JH (1996). Central neural control of
580 respiration and circulation during exercise. **Supplement 29**, 333–380.
- 581 Winkler AM, Ridgway GR, Webster MA, Smith SM & Nichols TE (2014). Permutation
582 inference for the general linear model. *NeuroImage* **92**, 381–397.
- 583 Woolrich MW, Behrens TEJ, Beckmann CF, Jenkinson M & Smith SM (2004). Multilevel linear
584 modelling for fMRI group analysis using Bayesian inference. *NeuroImage* **21**, 1732–1747.
- 585 Woolrich MW, Ripley BD, Brady M & Smith SM (2001). Temporal Autocorrelation in
586 Univariate Linear Modeling of fMRI Data. *NeuroImage* **14**, 1370–1386.
- 587

588
589
590
591
592

Tables

593 **Table 1.** Mean (\pm sd) physiological variables across conditioned respiratory tasks. *Significantly
594 ($p < 0.05$) different from sedentary group. Abbreviations: $P_{ET}CO_2$, pressure of end-tidal carbon
595 dioxide; $P_{ET}O_2$, pressure of end-tidal oxygen; RVT, respiratory volume per unit time.

	Unloaded breathing		Anticipation		Breathlessness	
	ATHLETE	SEDENTARY	ATHLETE	SEDENTARY	ATHLETE	SEDENTARY
Avg mouth pressure (cmH ₂ O)	0.54 (0.84)	0.15 (0.65)	0.71 (1.03)	0.21 (0.69)	6.22 (3.38)	5.17 (2.60)
$P_{ET}CO_2$ (mmHg)	35.96 (5.56)	35.08 (3.20)	35.50 (5.81)	34.76 (3.60)	36.34 (6.23)	35.40 (3.92)
$P_{ET}O_2$ (mmHg)	129.68 (6.41)	134.09 (15.15)	129.55 (6.75)	133.59 (13.47)	131.18 (6.83)	137.55 (16.42)
Respiratory rate (min ⁻¹)	10.15 (2.59)*	13.35 (3.51)	9.99 (2.63)*	12.93 (4.29)	9.40 (3.58)	11.54 (5.11)
RVT (% change from baseline)	-4.06 (5.70)	-0.56 (7.94)	-0.03 (12.14)	6.07 (18.78)	-20.00 (24.88)	-13.23 (28.54)

596
597
598
599
600

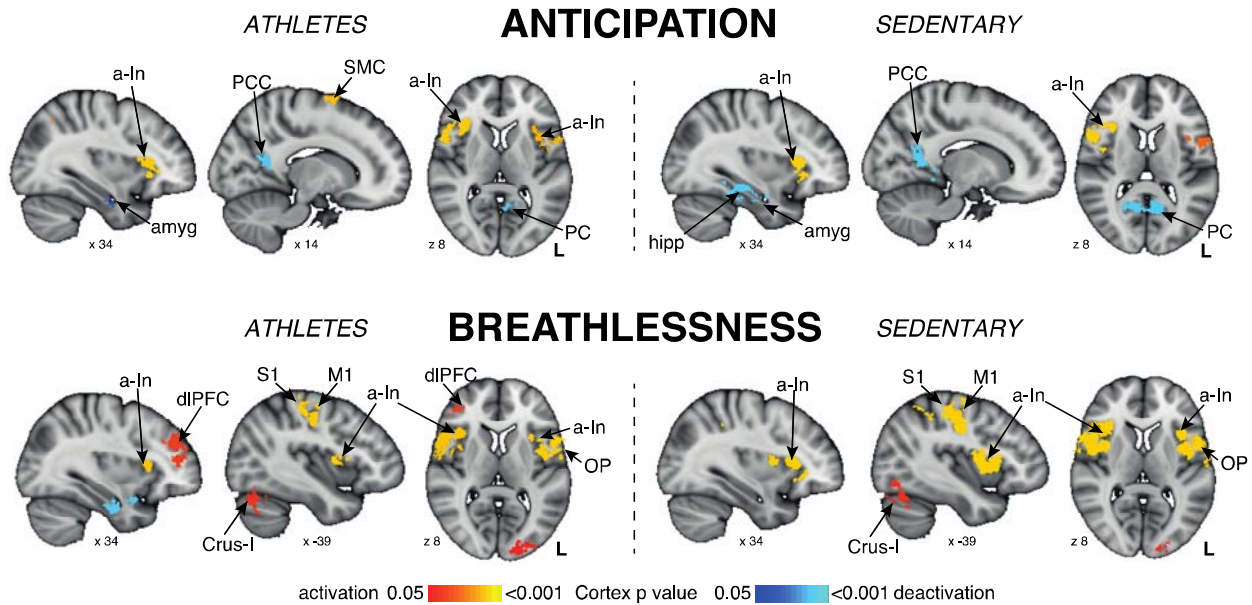
601 **Table 2.** Mean (\pm sd) physiological and psychological variables during breathlessness for both
602 athletes and sedentary subjects.

	ATHLETE	SEDENTARY
Peak mouth pressure (cmH ₂ O)	14.4 (8.5)	12.0 (5.8)
Breathlessness intensity rating (%)	46.3 (14.1)	46.7 (18.1)
Breathlessness anxiety rating (%)	31.9 (17.8)	36.1 (20.0)
Unloaded breathing intensity rating (%)	2.3 (3.5)	3.4 (3.4)
Unloaded breathing anxiety rating (%)	2.8 (4.8)	2.2 (2.7)

603

604
605
606
607
608

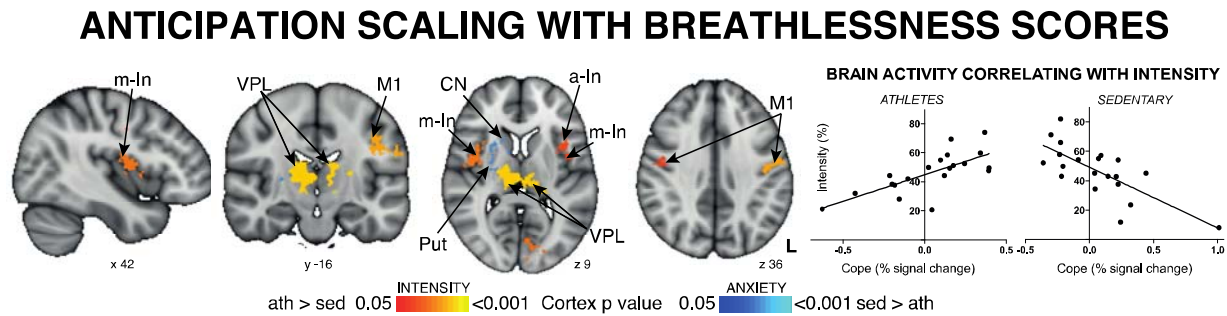
Figures



609
610

611 **Figure 1. Mean BOLD activity in athletes and sedentary controls.** Top: BOLD activity
612 during conditioned anticipation of breathlessness. Bottom: BOLD activity during a
613 breathlessness challenge, induced via inspiratory resistive loading. The images consist of a
614 colour-rendered statistical map superimposed on a standard (MNI 1x1x1 mm) brain, and
615 significant regions are displayed with a non-parametric cluster probability threshold of $t < 3.1$; p
616 < 0.05 (corrected for multiple comparisons). Abbreviations: M1, primary motor cortex; SMC,
617 supplementary motor cortex; dACC, dorsal anterior cingulate cortex; PCC, posterior cingulate
618 cortex; dIPFC, dorsolateral prefrontal cortex; a-In, anterior insula; OP, operculum; amyg,
619 amygdala; hipp, hippocampus; Crus-I, cerebellar lobe; activation, increase in BOLD signal;
620 deactivation, decrease in BOLD signal.

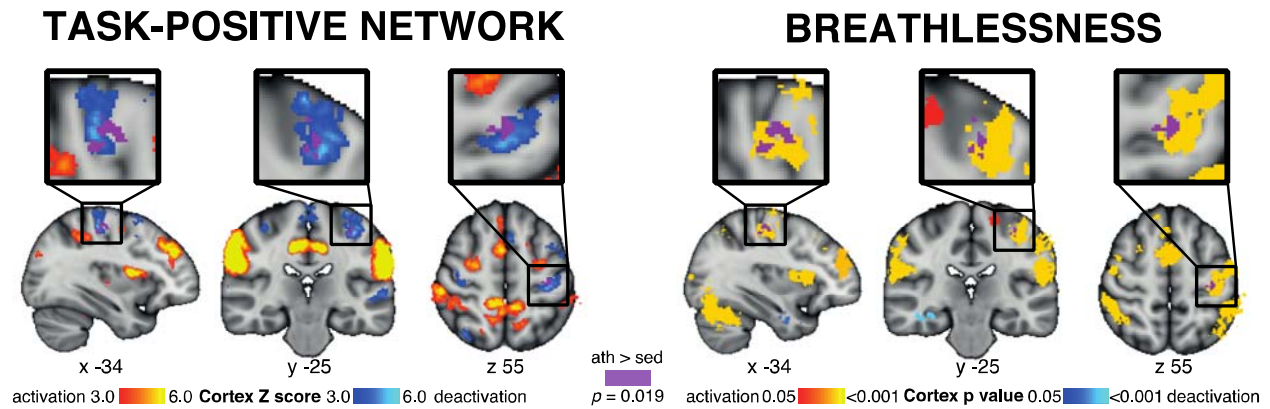
621
622
623
624
625



626
627

628 **Figure 2. Interaction between groups and breathlessness scores.** Left: BOLD activity during
629 conditioned anticipation of breathlessness. Red-yellow = BOLD activity correlating with
630 intensity scores in athletes > sedentary subjects; blue-light blue = BOLD activity correlating with
631 anxiety scores in sedentary > athletic subjects. Right: Percentage BOLD signal change within the
632 (red-yellow) intensity-correlated imaging mask against intensity scores, demonstrating a positive,
633 linear correlation in athletes and a negative relationship in sedentary subjects. The images consist
634 of a colour-rendered statistical map superimposed on a standard (MNI 1x1x1 mm) brain, and
635 significant regions are displayed with a non-parametric cluster probability threshold of $t < 3.1$; p
636 < 0.05 (corrected for multiple comparisons). Abbreviations: M1, primary motor cortex; a-In,
637 anterior insula; m-In, middle insula; hipp, hippocampus; put, putamen; CN, caudate nucleus;
638 VPL, ventral posterolateral thalamic nucleus. activation,

639
640
641
642



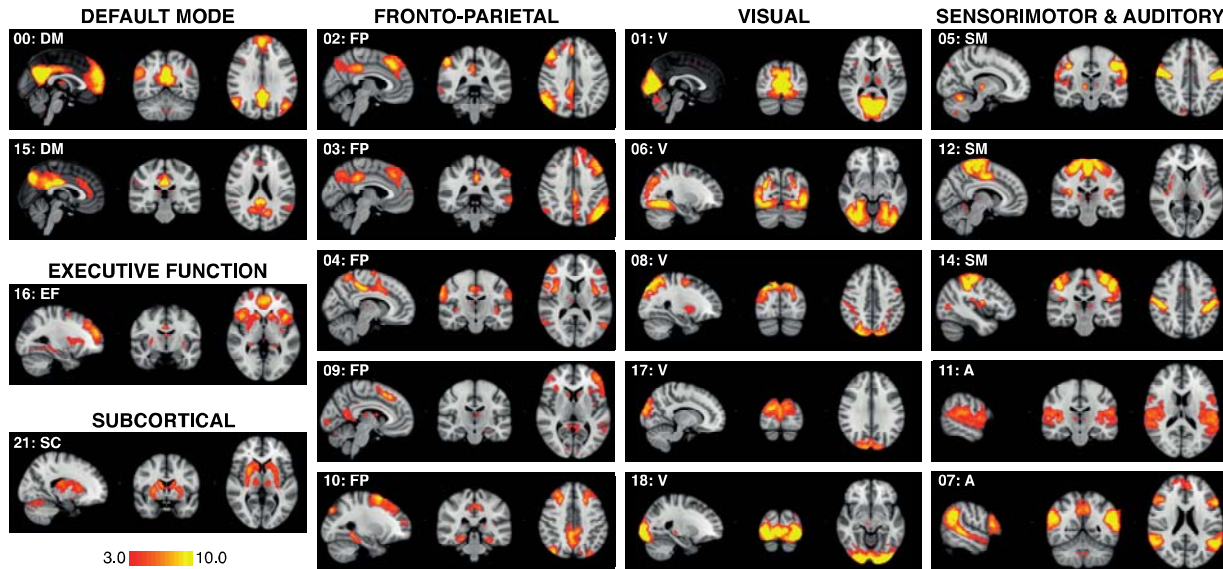
643
644
645
646
647
648
649
650
651

Figure 3. Differences in resting functional connectivity between athletes and sedentary subjects. Increased functional connectivity (purple) observed in athletes between an area of primary motor cortex that is active during breathlessness (right) and a cingulo-opercular task-positive network (left) identified at rest. The images consist of a colour-rendered statistical map superimposed on a standard (MNI 1x1x1 mm) brain, and significant regions are displayed with a non-parametric cluster probability threshold of $t < 3.1$; $p < 0.05$ (corrected for multiple comparisons).

652
653
654
655
656
657

SUPPLEMENTARY MATERIAL

Resting state networks



658
659
660
661
662
663
664

Supplementary Figure 1. Overview of the twenty resting state networks identified using independent-component analysis in 40 subjects, using a constrained dimensionality of 25 networks. The images consist of a colour-rendered statistical map superimposed on a standard (MNI 1x1x1 mm) brain.

665 **Finger opposition**

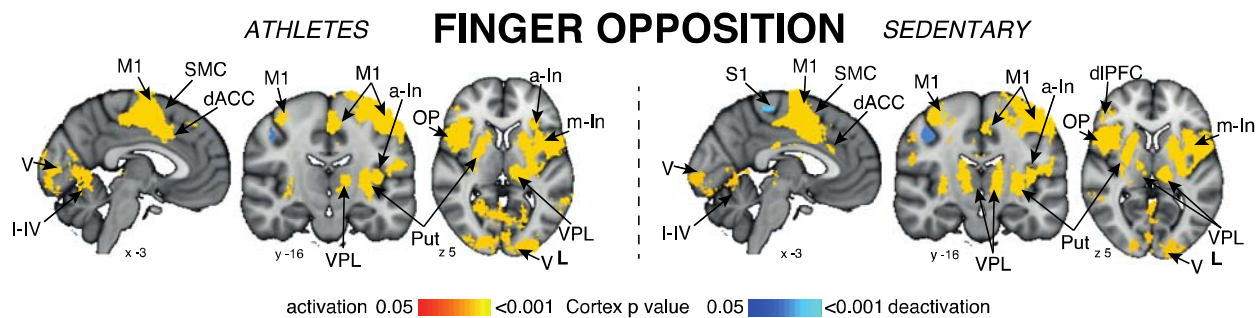
666

667 Finger opposition resulted in significant signal increases in both the brainstem and cortex in both
668 groups consistent with previous research (Pattinson *et al.*, 2009a; Faull *et al.*, 2015; 2016b), and
669 are presented in the Supplementary material. In sedentary subjects, significantly increased
670 BOLD activity was observed in the bilateral motor cortex (more extensive activation in the
671 contralateral left motor cortex), supplementary motor cortex, dorsal anterior cingulate and
672 paracingulate cortices, primary sensory cortex (more extensive activation in the contralateral left
673 sensory cortex), superior parietal lobule, anterior insula cortex, operculum, caudate nucleus,
674 putamen, left ventral posterolateral nucleus of the thalamus, bilateral cerebellum (VI and VIIIa
675 lobules) and (sedentary only) right dorsolateral prefrontal cortex and right ventral posterolateral
676 nucleus of the thalamus. Both subjects also revealed decreased BOLD activity in ipsilateral
677 sensory and motor cortices.

678

679

680



681

682

683 **Supplementary Figure 2.** Mean BOLD response to a finger opposition task in each of two
684 groups: 20 endurance athletes, and 20 age- and sex-matched sedentary control subjects. The
685 images consist of a colour-rendered statistical map superimposed on a standard (MNI 1x1x1
686 mm) brain, and significant regions are displayed with a non-parametric cluster probability
687 threshold of $t < 3.1$; $p < 0.05$ (corrected for multiple comparisons). Abbreviations: M1, primary
688 motor cortex; S1, primary sensory cortex; SMC, supplementary motor cortex; dACC, dorsal
689 anterior cingulate cortex; Put, putamen; dIPFC, dorsolateral prefrontal cortex; a-In, anterior
690 insula; m-In, middle insula; OP, operculum; V, visual cortex; I-IV, cerebellar lobe; VPL, ventral
691 posterolateral thalamic nucleus; activation, increase in BOLD signal; deactivation, decrease in
692 BOLD signal.